

Supporting Information

Highly Efficient Doping Titanium Dioxide with Sulfur using Disulfide-linked Macrocycles for Hydrogen Production under Visible Light

Meng Zhou,^a Xin Zhong,^a Dan Wei,^a Kang Yang,^a Yifan Chen,^a Chunman Jia,^{a,b,*} Jianwei Li^{a,b,c,*}

^a Hainan Provincial Key Laboratory of Fine Chem, School of Chemical Engineering and Technology, ^b One Health Institute, Hainan University, Haikou 570228, China.

^c MediCity Research Laboratory, University of Turku, Tykistökatu 6, Turku 20520, Finland.

* Corresponding authors: jianwei.li@utu.fi; jiachunman@hainanu.edu.cn

Contents

Fig. S1	Synthetic routes to the disulfide macrocycle (DSM).....	2
Fig. S2	¹ H NMR of 5-butoxybenzene-1,3-diol in CDCl ₃	2
Fig. S3	¹³ C NMR of 5-butoxybenzene-1,3-diol in CDCl ₃	3
Fig. S4	High resolution mass spectrum of 5-butoxybenzene-1,3-diol.	3
Fig. S5	¹ H NMR of O,O'-(5-butoxy-1,3-phenylene) bis (dimethylcarbamothioate) in CDCl ₃	3
Fig. S6	¹³ C NMR of O,O'-(5-butoxy-1,3-phenylene) bis (dimethylcarbamothioate) in CDCl ₃	4
Fig. S7	High resolution mass spectrum of O,O'-(5-butoxy-1,3-phenylene) bis (dimethylcarbamothioate).	4
Fig. S8	¹ H NMR of S,S'-(5-butoxy-1,3-phenylene) bis(dimethylcarbamothioate) in CDCl ₃	4
Fig. S9	¹³ C NMR of S,S'-(5-butoxy-1,3-phenylene) bis(dimethylcarbamothioate) in CDCl ₃	5
Fig. S10	High resolution mass spectrum of S,S'-(5-butoxy-1,3-phenylene) bis(dimethylcarbamothioate).	5
Fig. S11	¹ H NMR of 5-butoxybenzene-1,3-dithiol in CDCl ₃	5
Fig. S12	¹³ C NMR of 5-butoxybenzene-1,3-dithiol in CDCl ₃	6
Fig. S13	High resolution mass spectra of 5-butoxybenzene-1,3-dithiol.	6
Fig. S14	¹ H NMR of the disulfide macrocycle (DSM) in CDCl ₃	6
Fig. S15	¹³ C NMR of the disulfide macrocycle (DSM) in CDCl ₃	7
Fig. S16	High resolution mass spectrum of the disulfide macrocycle (DSM).....	7
Fig. S17	Synthesis flow chart of DSM-TiO ₂ system materials.....	7
Fig. S18	SEM、 EDX and elemental mapping of DSM-TiO ₂ (5.0 wt%)......	8
Fig. S19	The EDX analysis of the Pt/DSM-TiO ₂ (5.0 wt%)......	8
Fig. S20	The physical absorption and desorption measured of native TiO ₂ and DSM-TiO ₂ (2.5/5.0/7.5 wt%).....	9
Fig. S21	Pore distribution of native TiO ₂ and DSM-TiO ₂ (2.5/5.0/7.5 wt%)......	9
Fig. S22	Thermogravimetric analysis of DSM and DSM-TiO ₂ (7.5 wt%) materials.	10
Fig. S24	X-ray photoelectron spectra of DSM-TiO ₂ (5.0 wt%).	11
Fig. S25	The solid UV-vis spectrum of DSM-TiO ₂ (2.5\5.0\7.5 wt%)......	12
Fig. S26	Hydrogen production performance of DSM-TiO ₂ (5.0 wt%) calcined at different temperatures.....	12
Fig. S27	Hydrogen production performance of native TiO ₂ and DSM-TiO ₂ (2.5/5.0/7.5 wt%)	13
Fig. S28	Hydrogen production performance of DSM-TiO ₂ with different metal.	13
Fig. S29	XPS and XRD maps after the 50 hours cycle stability experiment of Pt(0.3 wt%)/DSM-TiO ₂ (5.0 wt%)....	14
Fig. S30	Solid steady state fluorescence spectrum of native TiO ₂ and DSM-TiO ₂ (2.5/5.0/7.5 wt%)......	15
Fig. S31	Density Functional theory (DFT) computes the structural model.	15
Table. S1	Pt and S contents in DSM-TiO ₂ (5.0 wt%)......	16
Table. S2	Specific surface area、 pore size and pore volume of native TiO ₂ and DSM-TiO ₂ materials	16
Table. S3	The apparent quantum yield of DSM-TiO ₂ (5.0 wt%) materials.	16

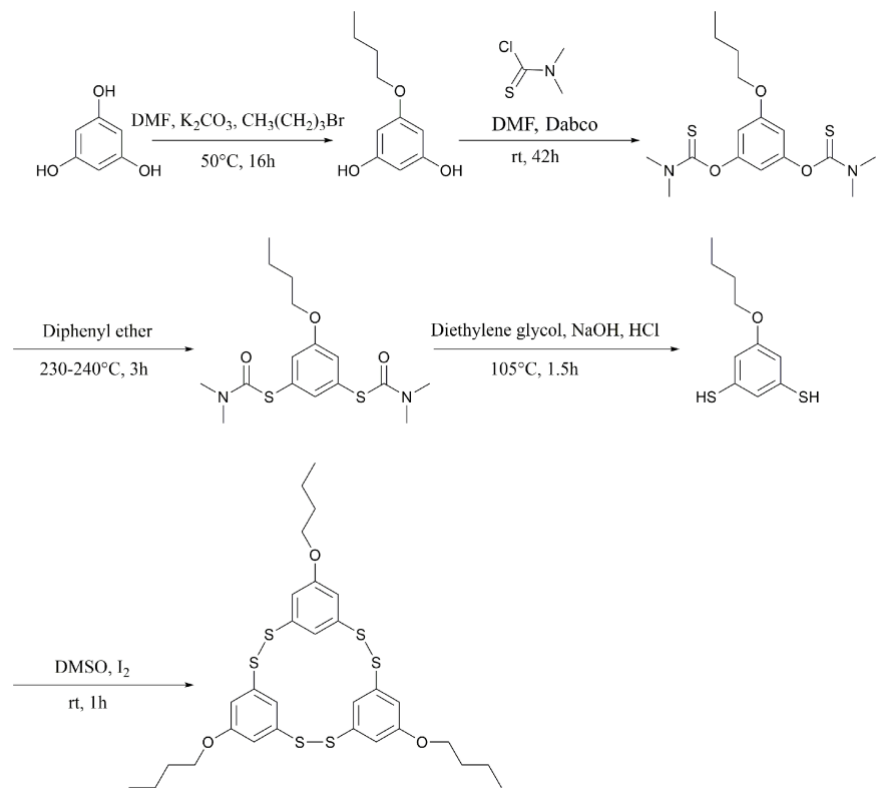


Fig. S1 Synthetic routes to the disulfide macrocycle (DSM).

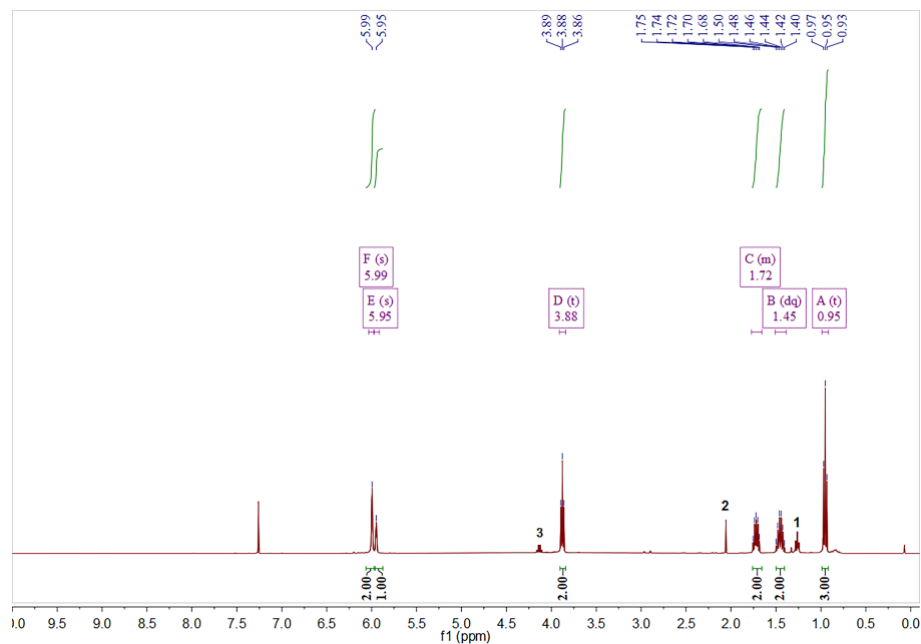


Fig. S2 1H NMR of 5-butoxybenzene-1,3-diol in $CDCl_3$, in which the peaks 1, 2, 3 are assigned to the residual solvent ethyl acetate.

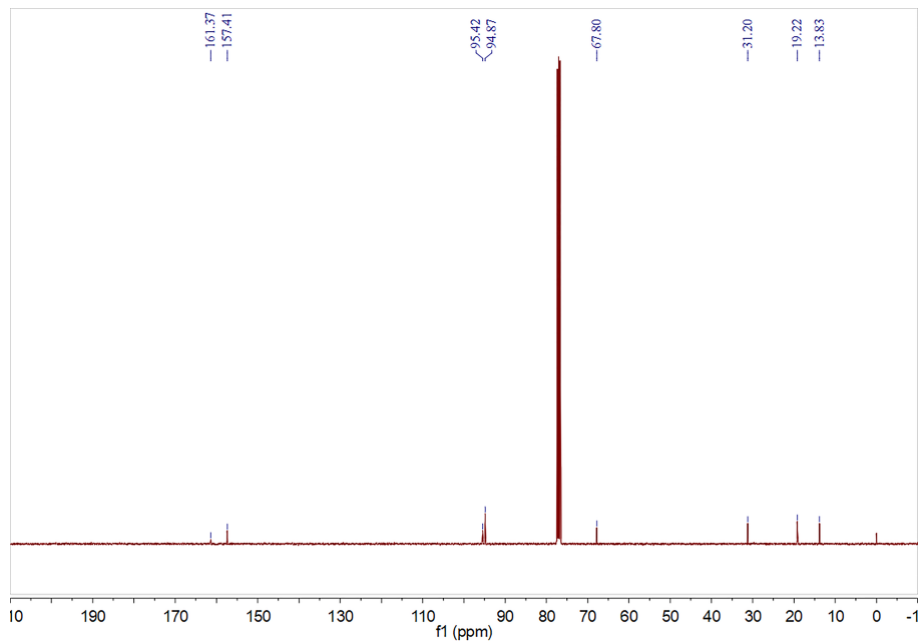


Fig. S3 ^{13}C NMR of 5-butoxybenzene-1,3-diol in CDCl_3 .

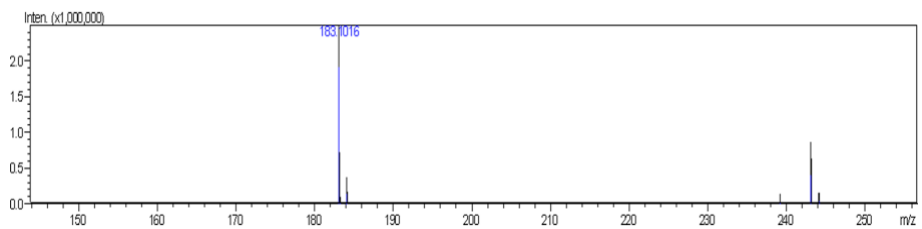


Fig. S4 High resolution mass spectrum of 5-butoxybenzene-1,3-diol.

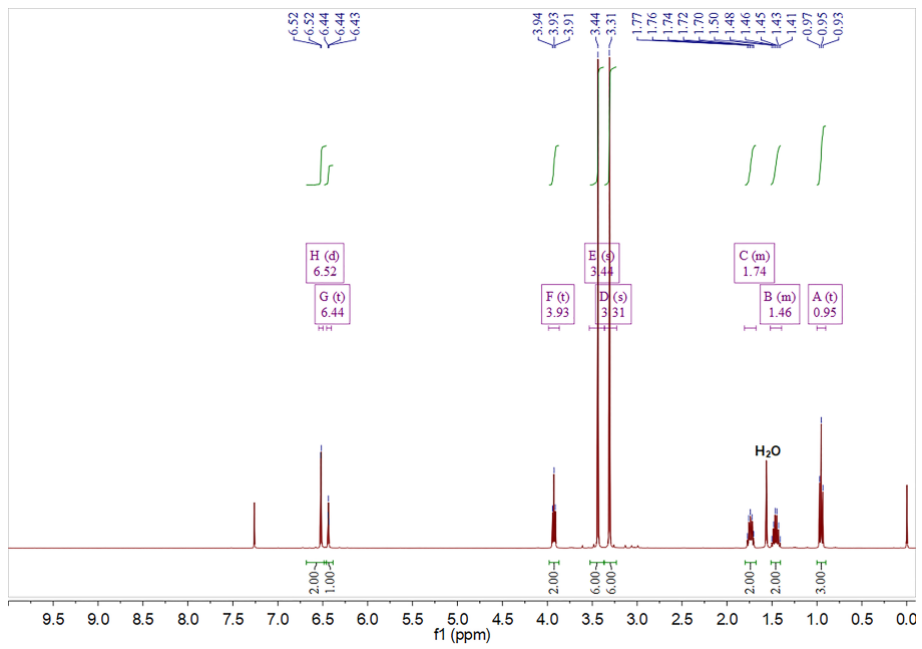


Fig. S5 ^1H NMR of O,O'-(5-butoxy-1,3-phenylene) bis (dimethylcarbamothioate) in CDCl_3 .

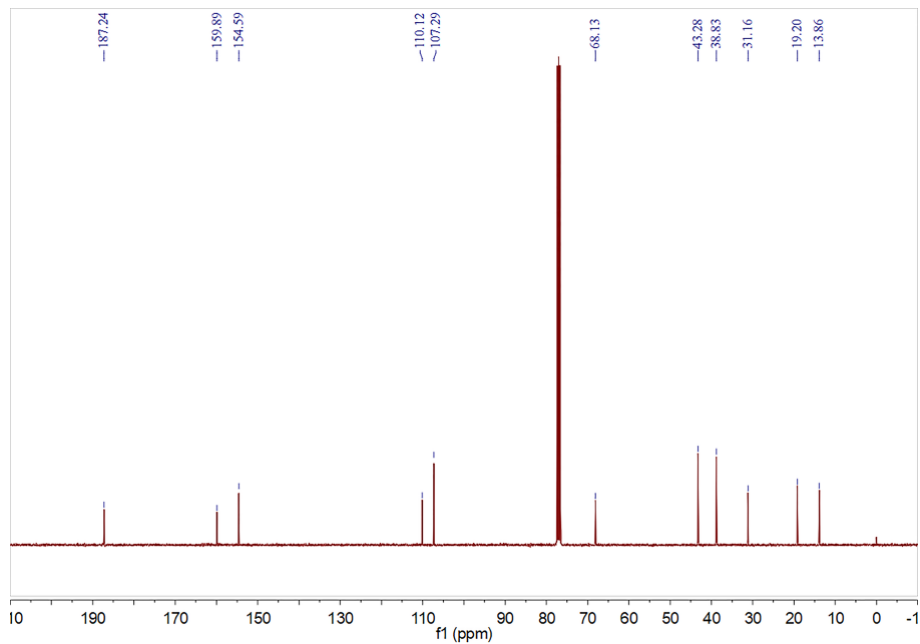


Fig. S6 ^{13}C NMR of O,O'-(5-butoxy-1,3-phenylene) bis (dimethylcarbamothioate) in CDCl_3 .

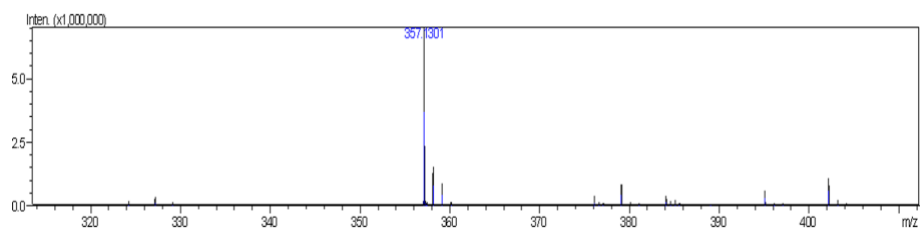


Fig. S7 High resolution mass spectrum of O,O'-(5-butoxy-1,3-phenylene) bis (dimethylcarbamothioate).

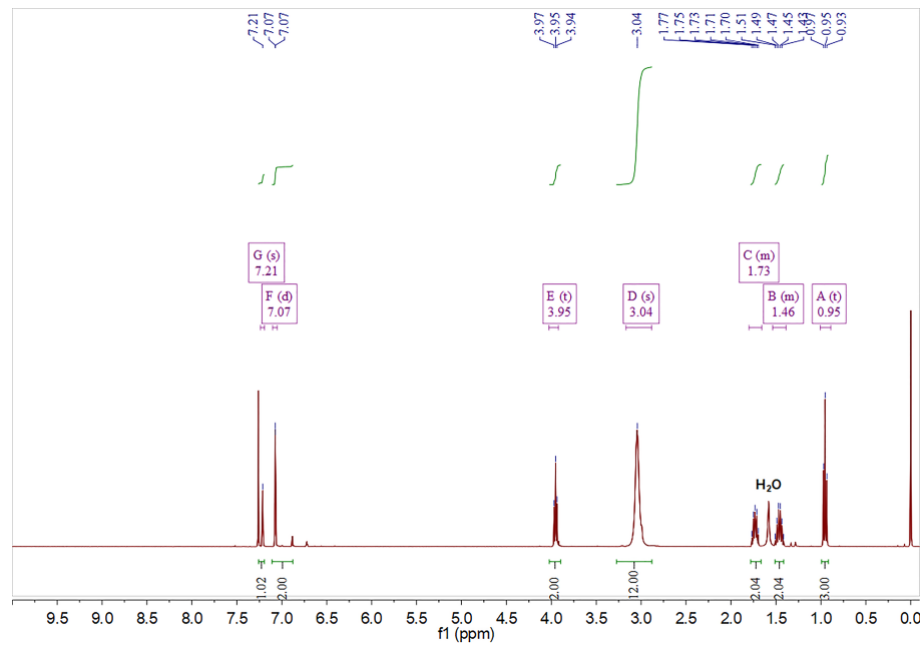


Fig. S8 ^1H NMR of S,S'-(5-butoxy-1,3-phenylene) bis(dimethylcarbamothioate) in CDCl_3 .

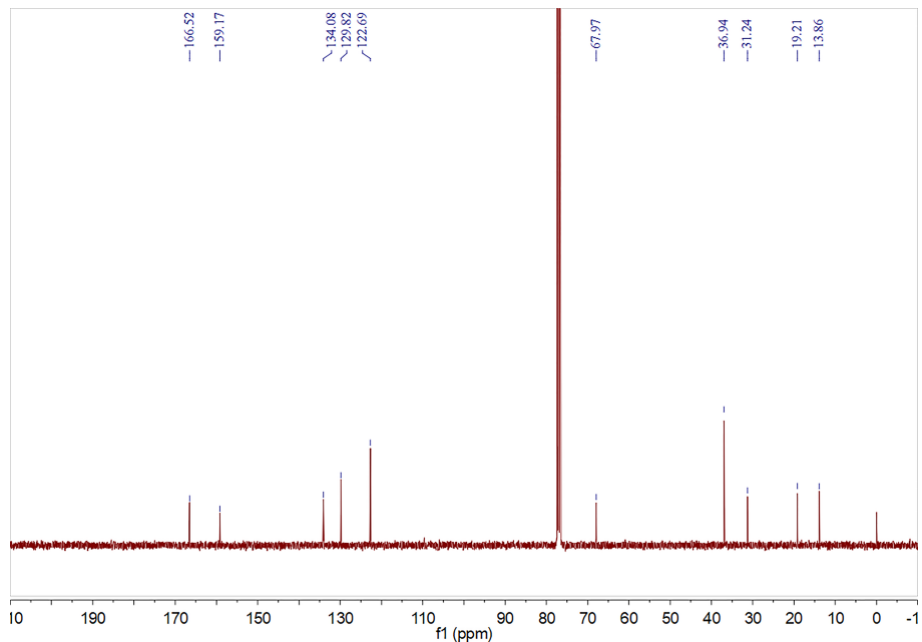


Fig. S9 ^{13}C NMR of S,S'-(5-butoxy-1,3-phenylene) bis(dimethylcarbamothioate) in CDCl_3 .

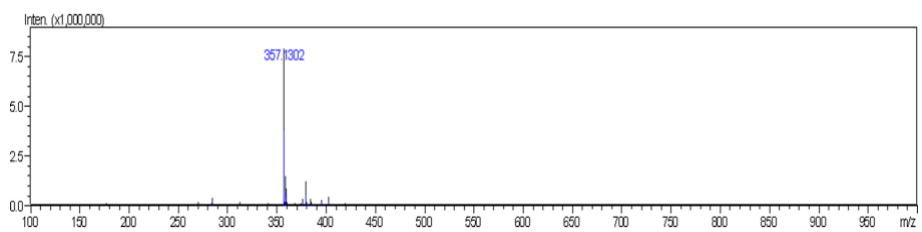


Fig. S10 High resolution mass spectrum of S,S'-(5-butoxy-1,3-phenylene) bis(dimethylcarbamothioate).

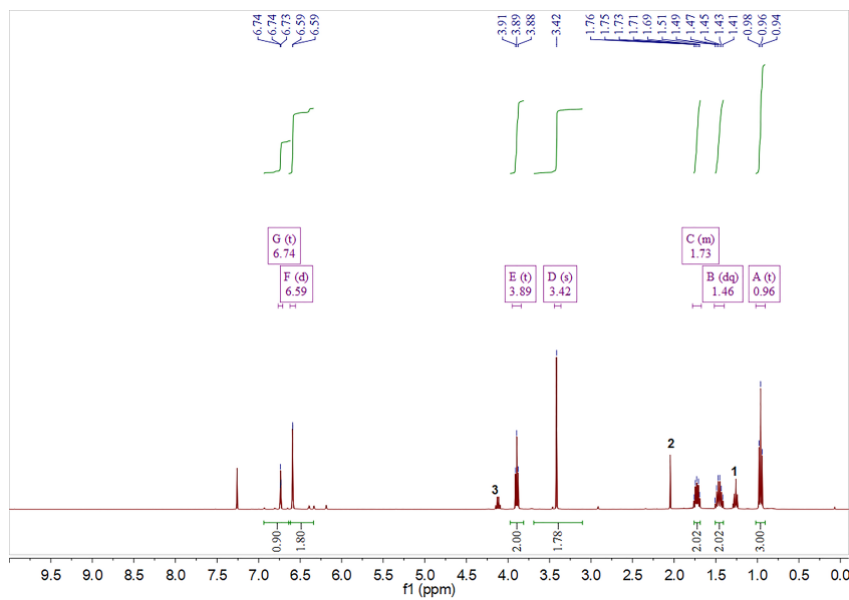


Fig. S11 ^1H NMR of 5-butoxybenzene-1,3-dithiol in CDCl_3 , in which the peaks 1, 2, 3 are assigned to the residual solvent ethyl acetate.

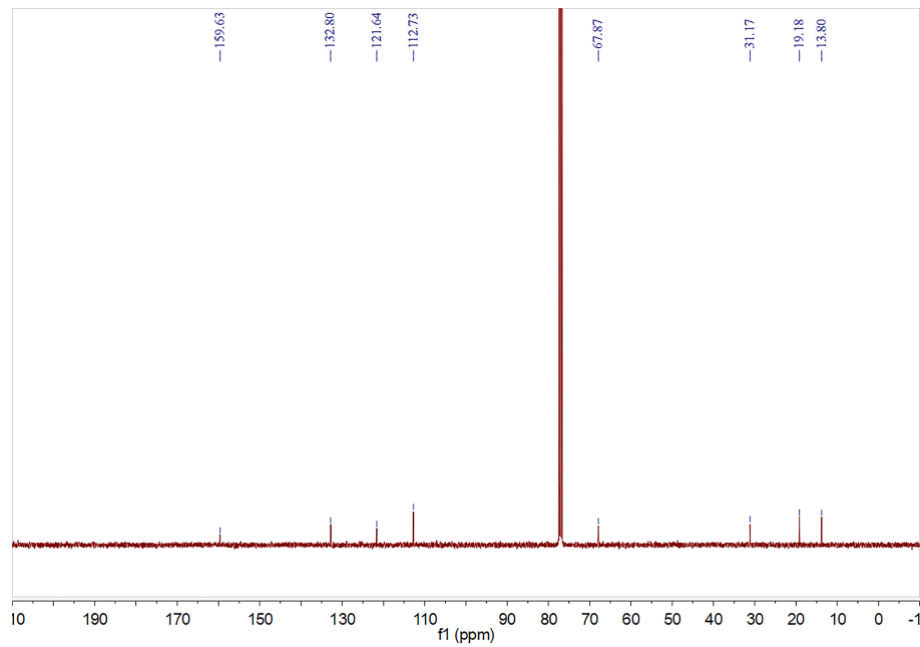


Fig. S12 ^{13}C NMR of 5-butoxybenzene-1,3-dithiol in CDCl_3 .

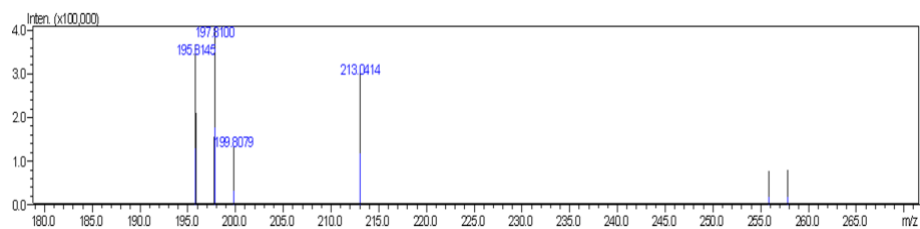


Fig. S13 High resolution mass spectra of 5-butoxybenzene-1,3-dithiol.

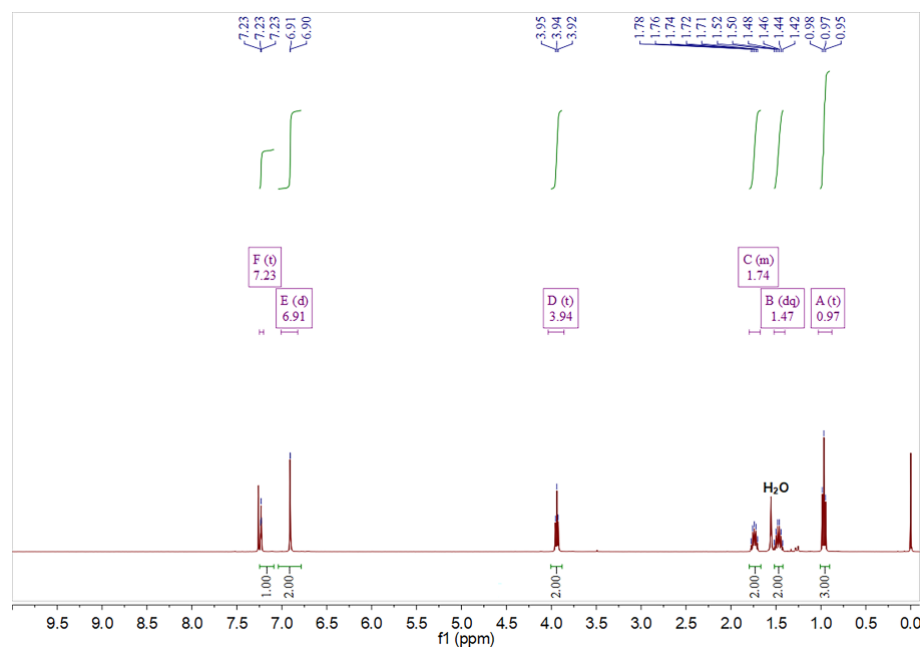


Fig. S14 ^1H NMR of the disulfide macrocycle (DSM) in CDCl_3 .

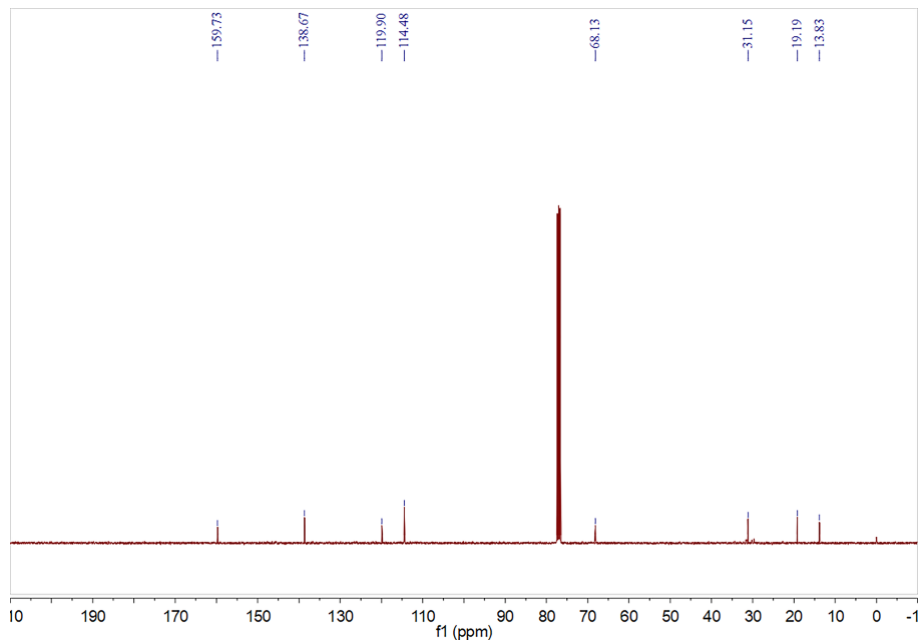


Fig. S15 ^{13}C NMR of the disulfide macrocycle (DSM) in CDCl_3 .

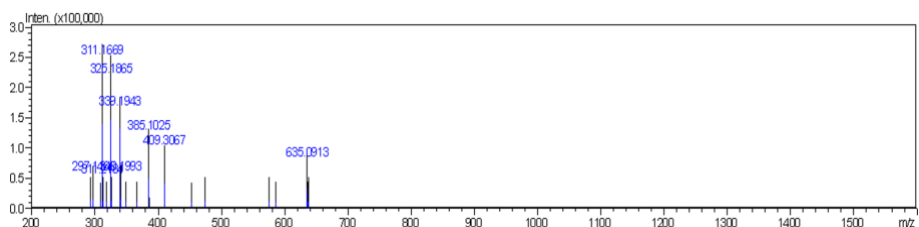


Fig. S16 High resolution mass spectrum of the disulfide macrocycle (DSM).

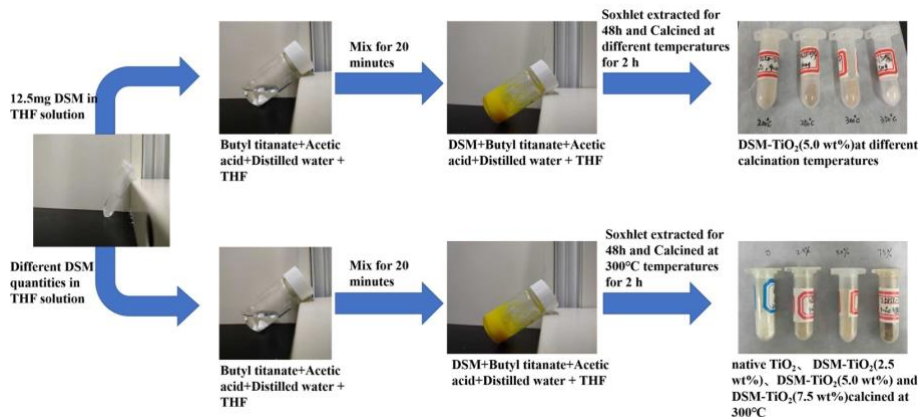


Fig. S17 DSM-TiO₂(5.0 wt%) at different calcination temperatures and DSM-TiO₂ with different DSM content (native TiO₂、DSM-TiO₂(2.5 wt%)、DSM-TiO₂(5.0 wt%)、DSM-TiO₂(7.5 wt%)) at 300°C were synthesized.

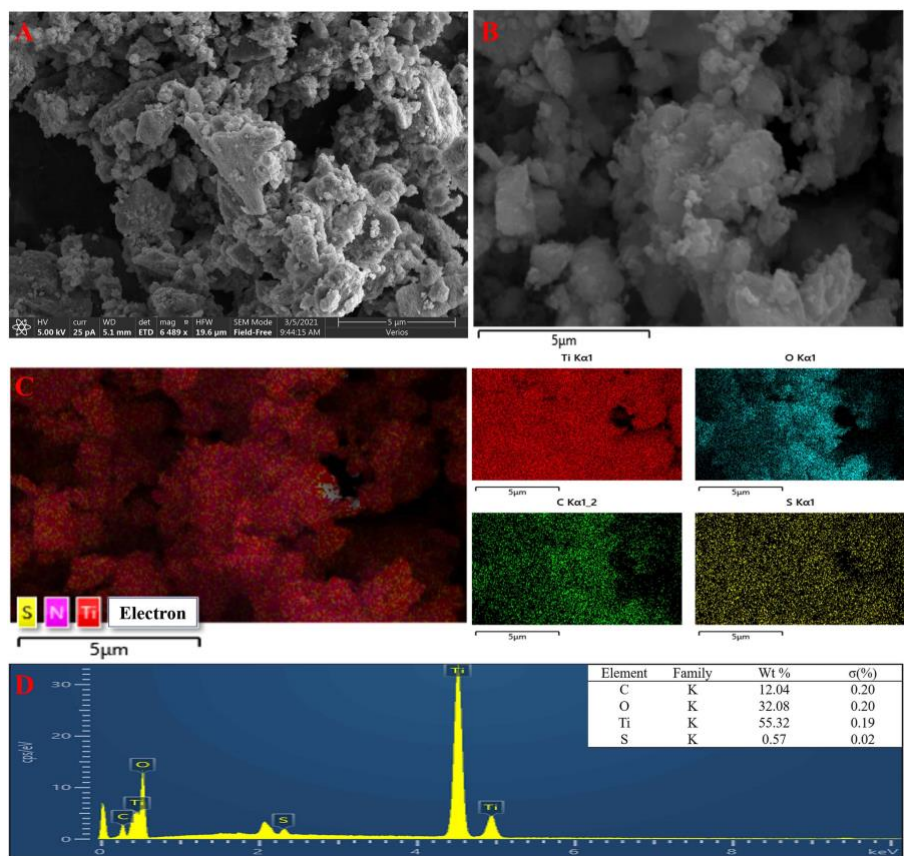


Fig. S18 (A) and (B) SEM, (C) the elemental mapping image, and (D) EDX analysis of DSM-TiO₂(5.0 wt%).

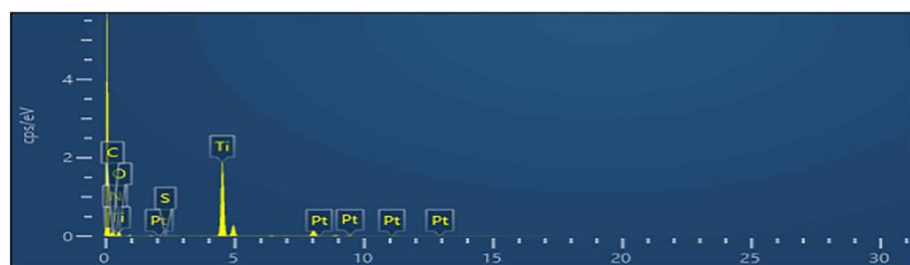


Fig. S19 The EDX analysis of the Pt/DSM-TiO₂(5.0 wt%).

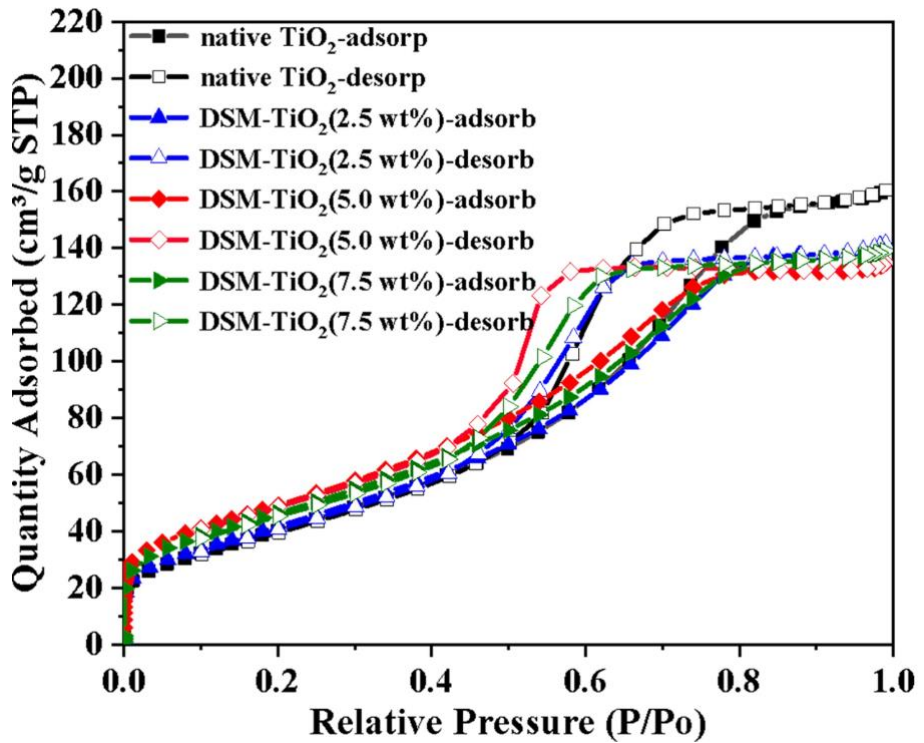


Fig. S20 The physical absorption and desorption measured at 77K of native TiO_2 and DSM- TiO_2 (2.5/5.0/7.5 wt%).

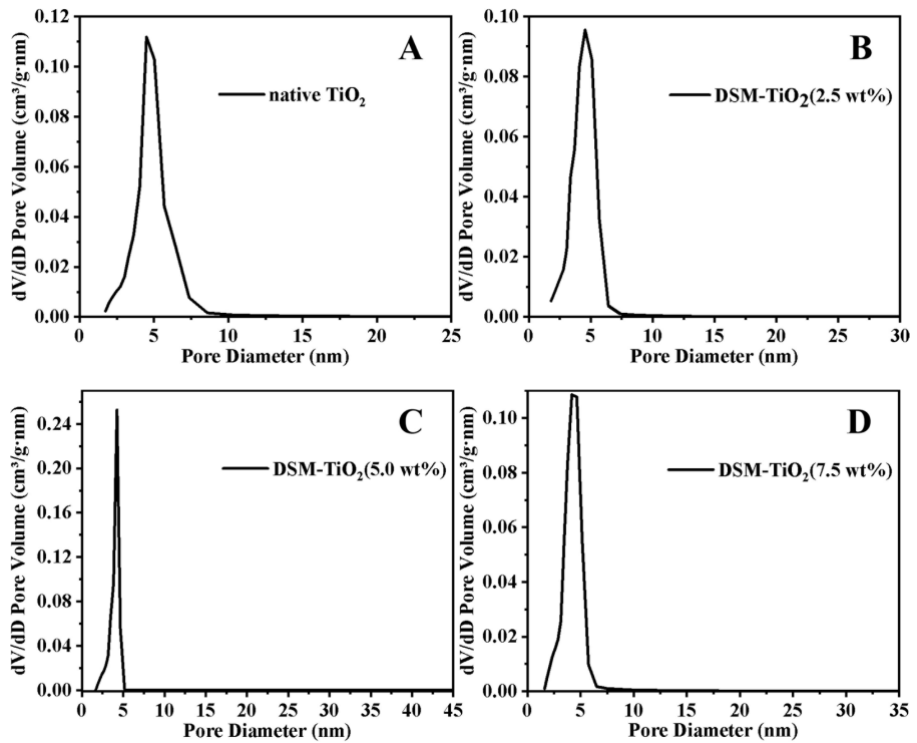


Fig. S21 Pore distribution of native TiO_2 and DSM- TiO_2 (2.5/5.0/7.5 wt%).

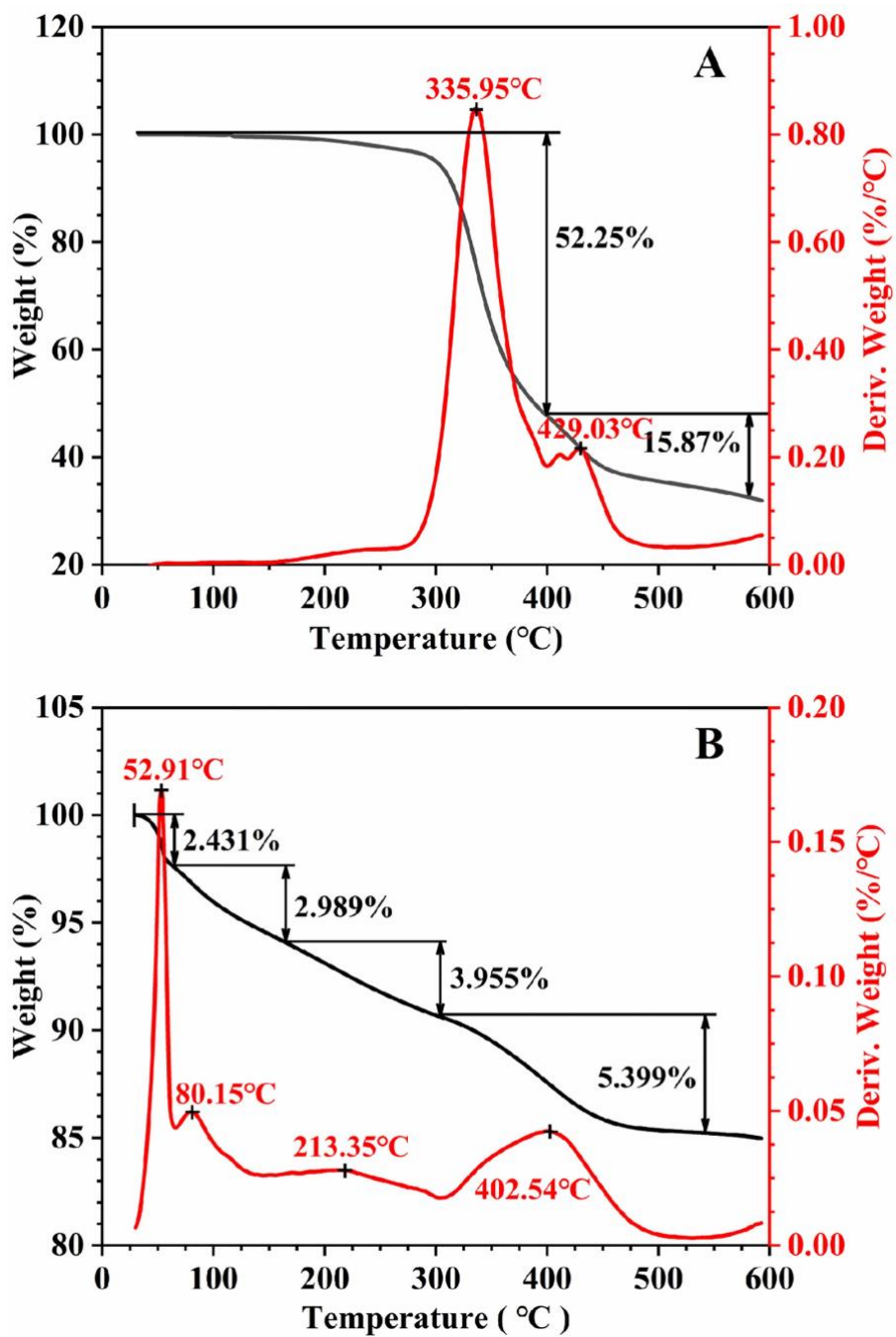


Fig. S22 Thermogravimetric analysis of (A) DSM and (B) DSM-TiO₂(7.5 wt%) materials. The temperature gradient was from room temperature to 600°C at a heating rate at 10 °C/min.

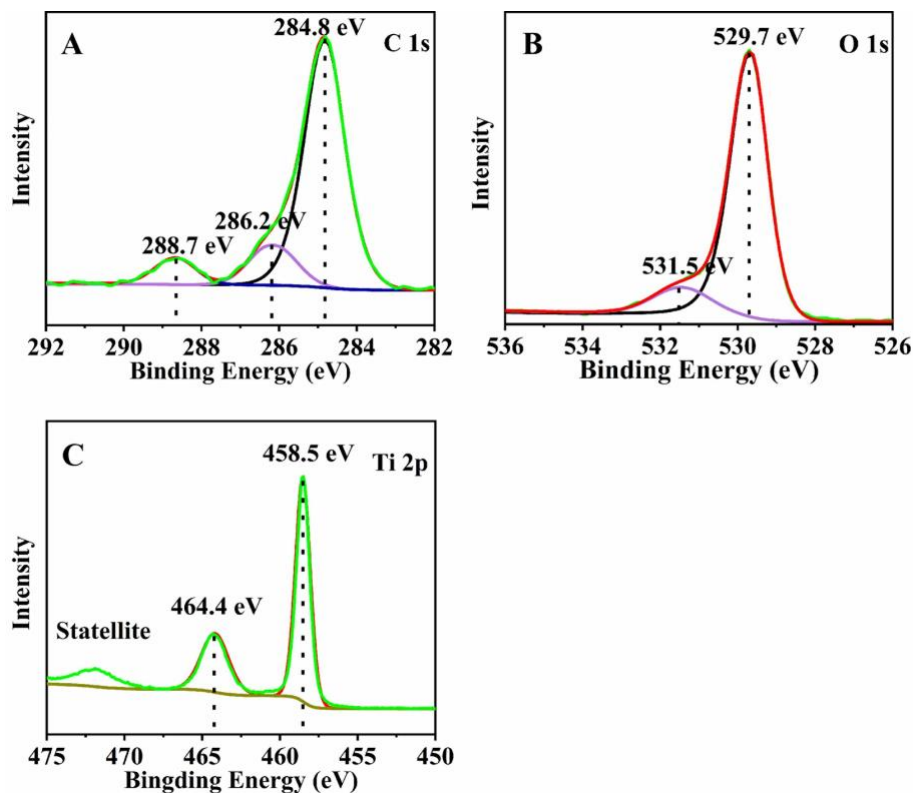


Fig. S23 X-ray photoelectron spectra for Ti and O of native TiO_2 . Atomic ratio of $\text{Ti} : \text{O} = 36\% : 63\% \approx 1 : 2$.

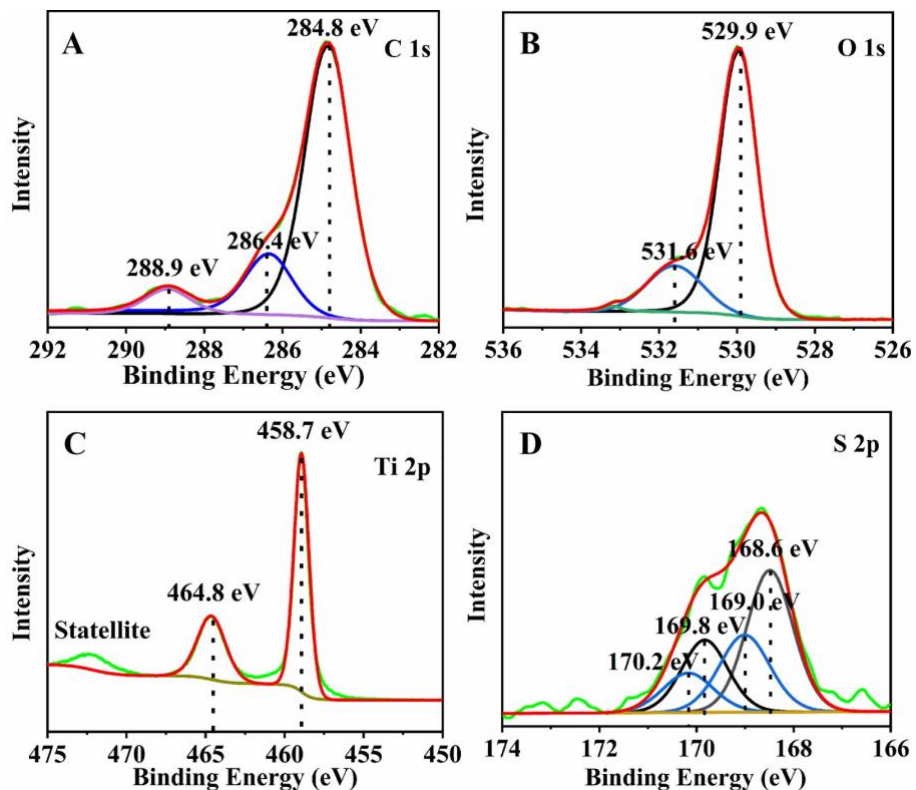


Fig. S24 X-ray photoelectron spectra for Ti, O and S of DSM- TiO_2 (5.0 wt%). The weight ratio of $\text{Ti} : \text{O} : \text{S} = 50\% : 36\% : 2.0\%$; Atomic ratio of $\text{Ti} : \text{O} = 25\% : 53\% \approx 1 : 2$.

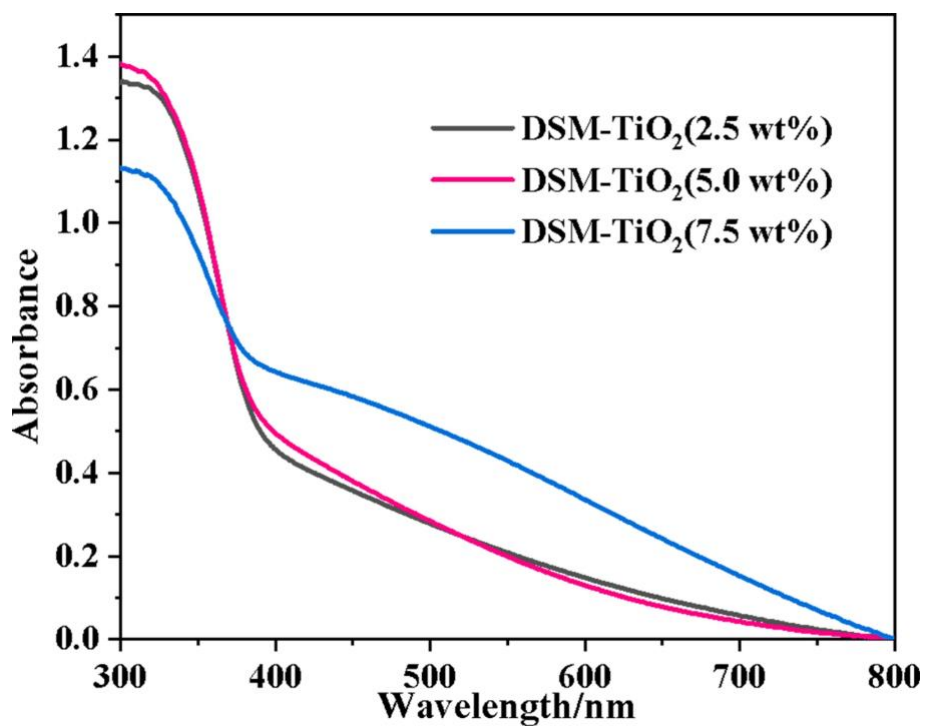


Fig. S25 The solid UV-vis spectrum of DSM-TiO₂(2.5\5.0\7.5 wt%).

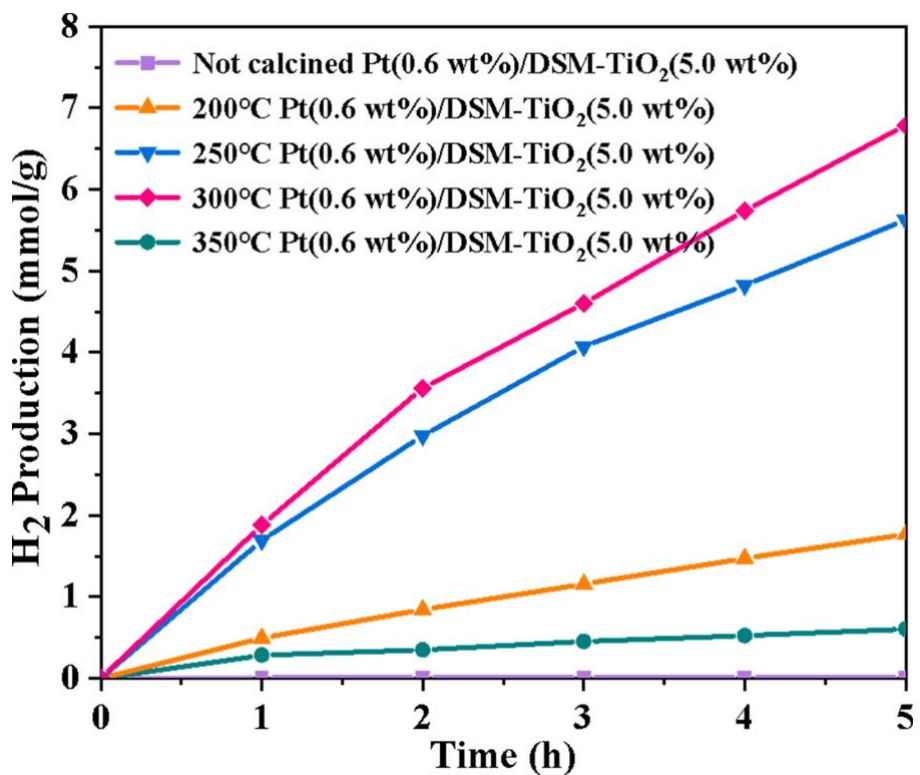


Fig. S26 Hydrogen production performance of DSM-TiO₂(5.0 wt%) calcined at different temperatures.

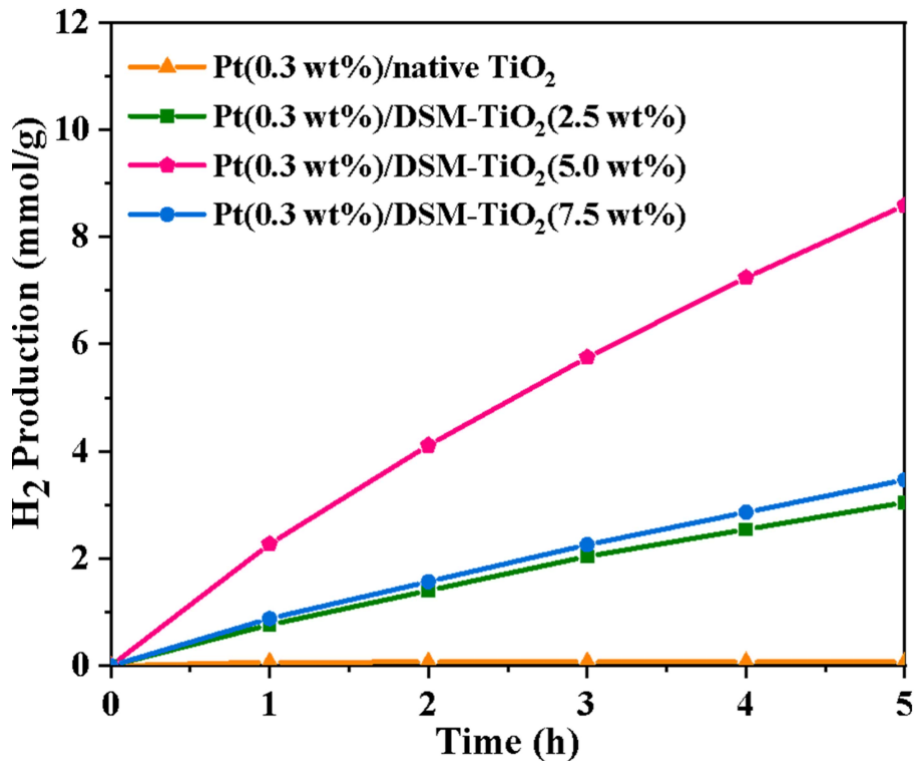


Fig. S27 Hydrogen production performance of DSM-TiO₂ with different dosages of DSM dopant.

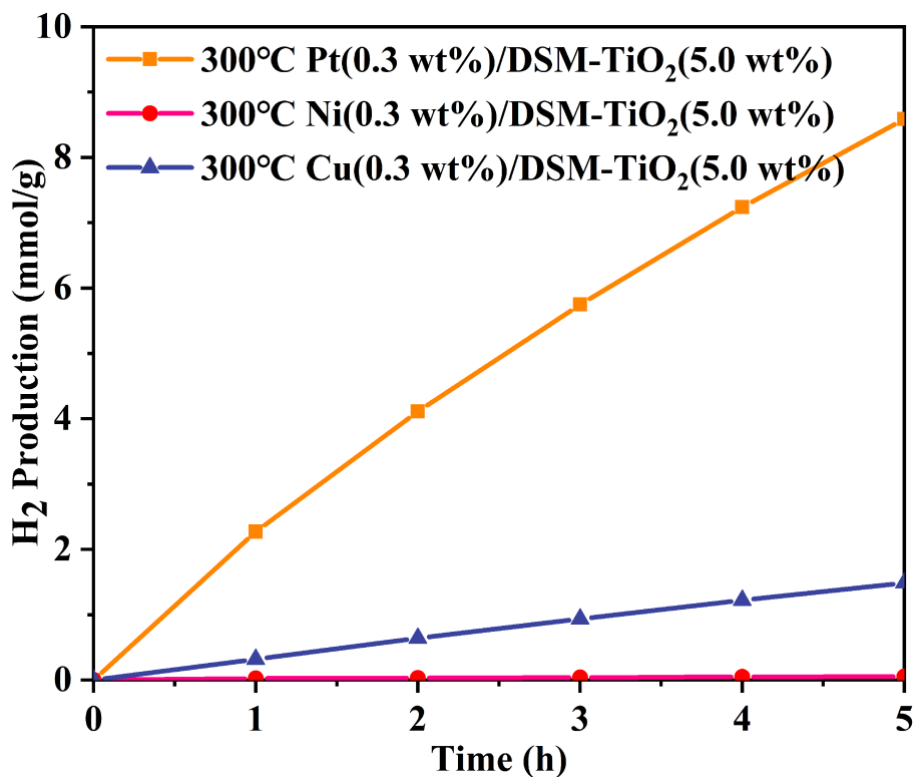


Fig. S28 Hydrogen production performance of DSM-TiO₂ with Pt, Ni and Cu.

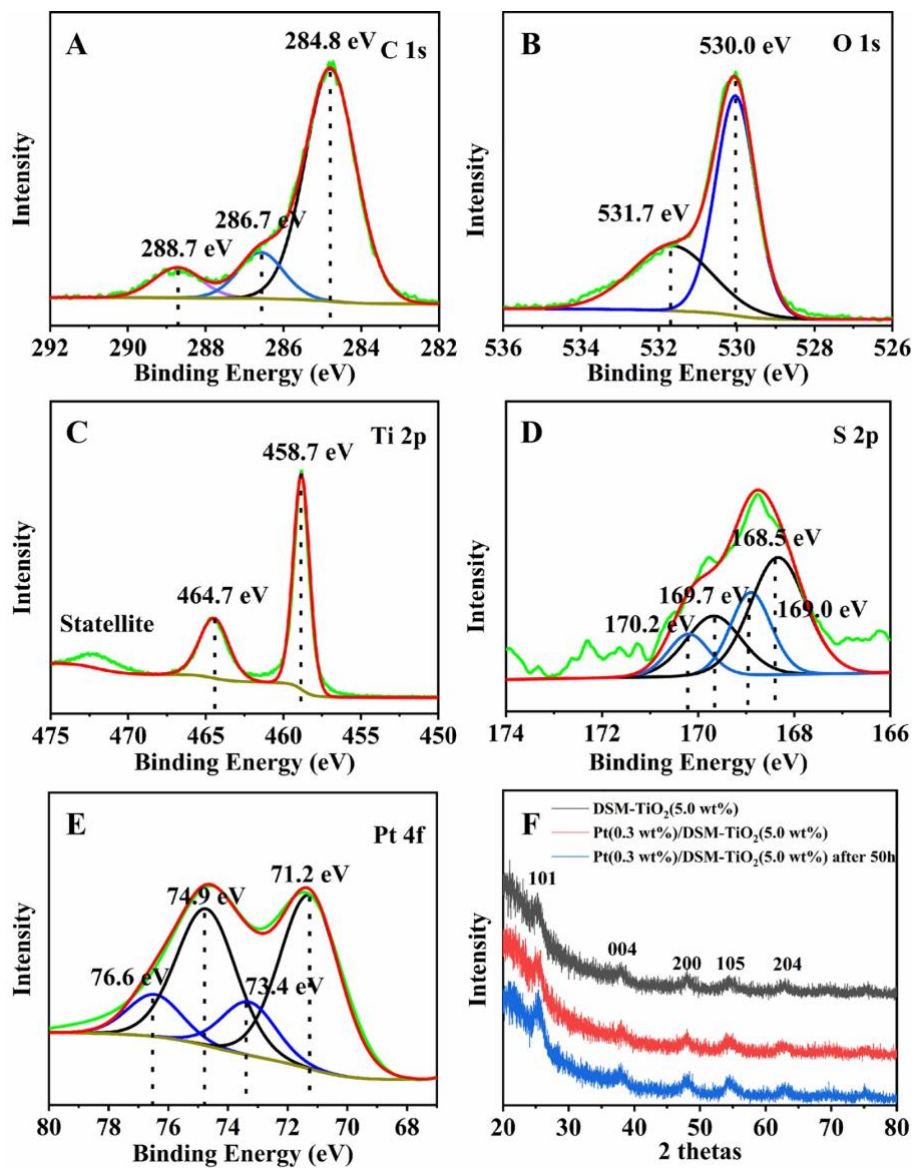


Fig. S29 XPS and XRD analysis of Pt(0.3 wt%)/DSM-TiO₂(5.0 wt%) after the 50 hours' cycle stability experiment.

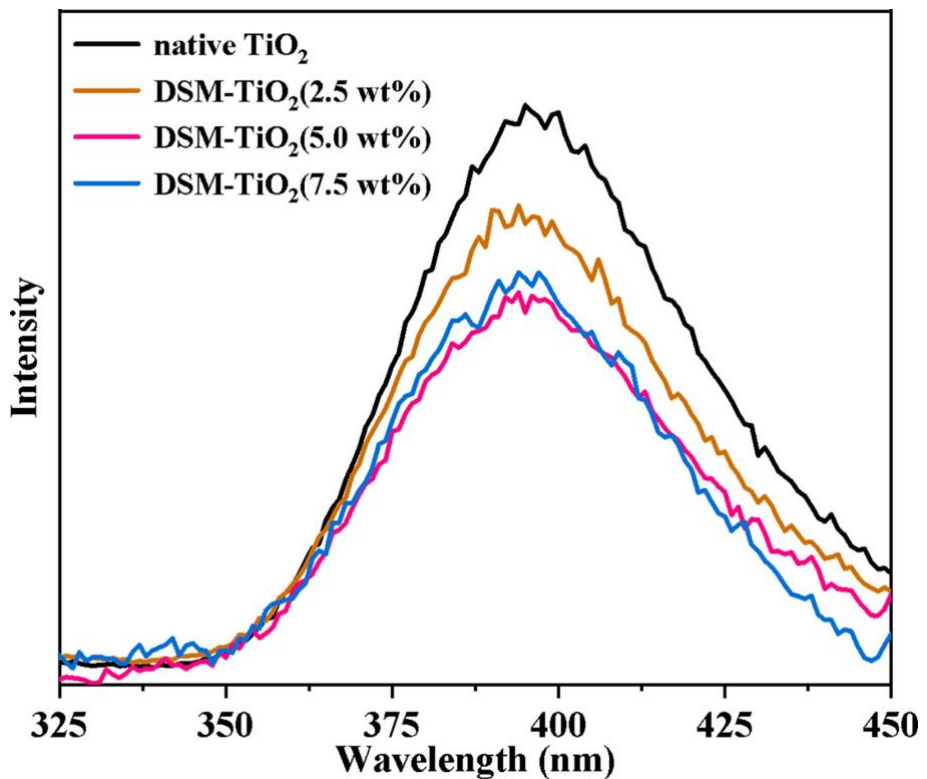


Fig. S30 Solid steady state fluorescence spectrum of native TiO₂ and DSM-TiO₂(2.5/5.0/7.5 wt%).

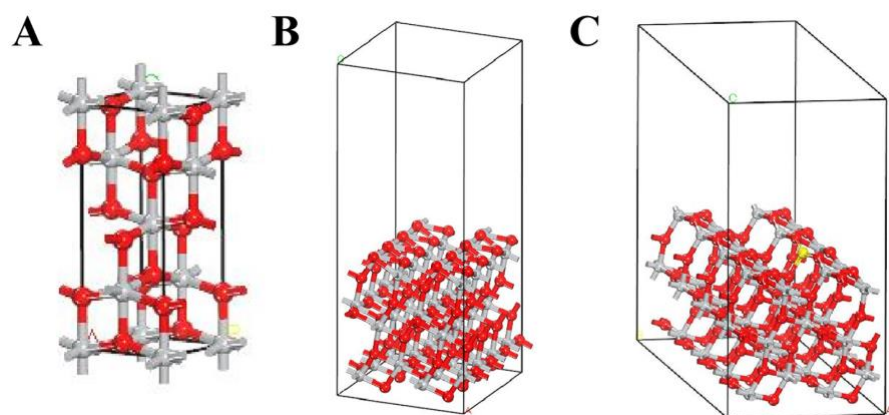


Fig. S31 Density Functional theory (DFT) computes the structural model: (A) Anatase TiO₂ cell, (B) Calculation model of anatase TiO₂, (C) Calculation model of S-TiO₂. Red is oxygen, silver is titanium, and yellow is sulfur.

Table. S1 Pt and S contents in DSM-TiO₂(5.0 wt%) analysed by ICP-AES.

Sample	Pt content (wt%)
Pt(0.3 wt%)/DSM-TiO ₂ (5.0 wt%)	0.3
Pt(0.6 wt%)/DSM-TiO ₂ (5.0 wt%)	0.5
Pt(1.0 wt%)/DSM-TiO ₂ (5.0 wt%)	0.8
Pt(1.5 wt%)/DSM-TiO ₂ (5.0 wt%)	1.4
Pt(2.0 wt%)/DSM-TiO ₂ (5.0 wt%)	2.0
Sample	S content (wt%)
DSM-TiO ₂ (5.0 wt%)	1.5

Table. S2 Specific surface area, pore size and pore volume of native TiO₂ and DSM-TiO₂ materials measured by adsorption isotherm at 77K.

Sample	Surface area (m ² /g)	Pore size (nm)	Pore volume (cm ³ /g)
native TiO ₂	154.73	4.80	0.252
DSM-TiO ₂ (2.5 wt%)	159.08	5.40	0.219
DSM-TiO ₂ (5.0 wt%)	181.07	3.91	0.216
DSM-TiO ₂ (7.5 wt%)	172.44	4.20	0.221

Table. S3 The apparent quantum yield of 20mg DSM-TiO₂(5.0 wt%) material that was irradiated under 405 nm and 450 nm LED lamps for 1 hour respectively.

Sample	Pt(0.3 wt%)/DSM-TiO ₂ (5.0 wt%)	Pt(0.3 wt%)/DSM-TiO ₂ (5.0 wt%)
Wavelength(nm)	405	450
AQY	1.15	0.64